

21



22 **Abstract**

23 Fjord sediments are recognized as hotspots for the burial and storage of organic carbon, yet
24 little is known about what drives the formation of these coastal carbon stores and how this has
25 altered over time. Here we show that fjords can act as sustained hotspots for carbon burial and
26 storage over Holocene timescales. Further we investigate the role of North Atlantic climate and
27 humans in the evolution of a coastal carbon store using sediment records from a temperate
28 Scottish fjord. Our findings indicate that climate and anthropogenic activity have
29 independently driven increases in terrestrial carbon to the marine environment. When both
30 these drivers were coupled, the terrestrial response was pronounced and the relative proportion
31 of terrestrial OC in the marine sediments increases from 5% up to 70%. We hypothesize that
32 sustained human disturbance through the late Holocene sensitized the catchment to abrupt
33 climate reorganizations. The results highlight the importance of fjords for carbon burial and
34 the significance of terrestrial carbon subsidy to the long-term carbon store.

35

36

37

38

39

40

41

42

43



44 **1. Introduction**

45 Early work suggested that fjords are location of high sediment deposition and that despite their
46 representation of a relatively small volume of the global continental margin ($<0.1\%$), they
47 contain $\sim 12\%$ of the sediments deposited over the past 100,000 yr (Syvitski et al. 1987). It was
48 also shown that fjords contain some of the highest organic carbon (OC) found in coastal
49 sediments (Skei, 1983), and that these systems may be global sink of OC - largely derived from
50 terrestrially materials (Burrell, 1988). Later work suggested that temperate fjords may contain
51 as much 12% of the global OC buried in margin sediments 100,000 yr (Newer and Keil, 2005),
52 in support of the previously estimated high global sediment deposition in the margin ($\sim 12\%$)
53 during this period (Syvitski et al. 1987). More recently, there has been a renewed interest in
54 the role of fjords as global hotspots for long-term carbon (C) burial (Hinjosa et al. 2014; Smith
55 et al. 2015; Cui et al. 2016a; Smeaton et al. 2016, 2017). To date, the mechanisms of enhanced
56 carbon burial in these systems, which are likely related to high productivity (Simo-Matchim et
57 al., 2016), rapid sedimentation (Syvitski et al., 1987), redox (Hinjosa et al. 2017), abundance
58 of mineral surfaces (Keil and Mayer, 2014), and inputs of terrestrial C from litter to petrogenic
59 materials) (Cui et al., 2016a, Smeaton and Austin, 2017) have yet to be fully explored.

60 In the North Atlantic region atmospheric forcing of Atlantic meridional overturning circulation
61 (AMOC), which is reflected by the strength and position of the North Atlantic Current (NAC),
62 coupled to persistent mode changes in the strength of the winter North Atlantic Oscillation
63 (NAO) (Thornalley et al. 2009; Ortega et al. 2015), is a plausible underlying climate forcing
64 mechanism that drives the sedimentary C composition of fjords during the post-deglacial
65 Holocene epoch (<11.5 ky) in Europe. In fact throughout the Holocene, decadal and millennial-
66 scale climatic variability has been well-documented in ice-core, marine sediment & terrestrial
67 archives (Meeker and Mayewski, 2002). In particular, North Atlantic Holocene archives are



amongst the most intensively studied records available, yet the climatic linkages between the ocean, atmosphere and terrestrial environment remain poorly understood on these timescales. Recently the impact of AMOC and NAO variability in the Holocene on terrestrial ecosystems sensitive to climate forcing (Seddon et al. 2016) has gained attention, the challenge lies in understanding the long-term interactions of climate and humans on C in the terrestrial environment and how this impacts the development of C stores at the land-ocean interface.

In the North Atlantic region previous attempts to separate the effects of climatic and human forcing on past alterations in terrestrial ecosystems have focused on the Baltic Sea (Zillén & Conley 2010); these authors showed that in the last two millennia hypoxic events mirrored the expansion and contraction of regional human population density, suggesting anthropogenic disturbance is a significant driver of coastal hypoxia through the introduction of terrestrial organic matter. While this work was successful in reconstructing the regional effects of humans and climate within the Baltic watershed and its C cycle, an aquatic repository situated farther to the west, should provide a more suitable location to investigate the link between humans and North Atlantic climate forcing. Fjord systems store C effectively due in part to their deep glacial geomorphology, high sedimentation rates and often low oxygenated bottom waters; these features make these systems ideal for reconstructing regional climate change (Cage & Austin 2010; Faust et al. 2016) while also accumulating stores of C (Smeaton et al. 2017). Scottish fjords have also been shown to be ideally situated for coupling to North Atlantic climate forcing (Austin et al. 2006; Gillibrand et al. 2005) due to their proximity to the major North Atlantic currents and the westerlies (Fig.1). Additionally, there are long regional records of human occupation and environmental disturbance (e.g. Smout. 1993; Tipping. 2013).

Here, we present a sediment record from Loch Sunart, a fjord on the west coast of Scotland (Fig.1) in an attempt to unravel the roles played by North Atlantic climate and human



92 disturbance play through the mid to late Holocene (7-0 ky) in the development of fjord
93 sedimentary C stores and the wider significance of long-term carbon burial.

94 2. Study Site

95 Loch Sunart is a temperate non-glaciated fjord on the west coast of Scotland (Fig.1). The fjord
96 is 30.7 km long and has an areal extent of 47.3 km² with a maximum depth of 145 m and
97 consists an outer, middle and upper basin separated by shallow rock sills at depths of 31m and
98 6m respectively. Loch Sunart's catchment covers 299 km² with the main tributaries, the rivers
99 Carnoch and Strontian entering close to the fjord head. The topographic nature of the catchment
100 results in rivers having flashy flow regimes (Gillibrand et al., 2005).

101 The oceanographic conditions of Loch Sunart and most other Scottish fjords result in well
102 ventilated bottom waters and generally they experience only minor seasonally hypoxic events
103 (Gillibrand et al., 2005). Recent calculations estimate the post-glacial sediments of Loch Sunart
104 hold 9.4 ± 0.2 Mt of OC (Smeaton et al., 2016), with an estimated 42.0 ± 10.1 % of the OC
105 held within the surface sediments being terrestrial in origin (Smeaton and Austin, 2017).

106 Loch Sunart's catchment is dominated by shallow (mean depth: 50cm) C-rich, peaty gley soil
107 and a land cover largely consisting of acid grasslands, commercial coniferous and deciduous
108 woodlands (Smeaton and Austin, 2017). The physical characteristics of Loch Sunart and its
109 catchment are largely representative of fjords across mainland Scotland (Smeaton et al. 2017);
110 further Syvitski and Shaw's (1995) table of generalised fjord characteristics indicates that the
111 fjords of mainland Scotland have comparable physical characteristics to the non-glaciated
112 fjords found on the Norwegian mainland, Canada and in New Zealand.

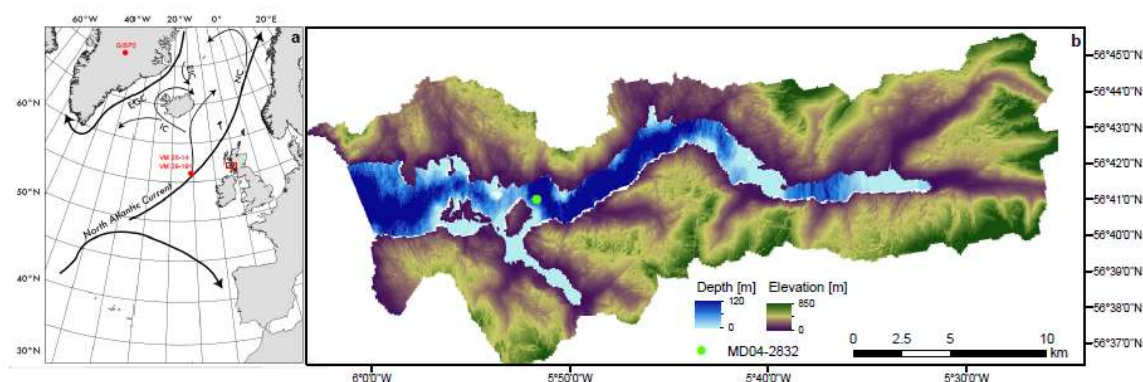


Figure.1 (a) North Atlantic Ocean circulation. Location of Loch Sunart (Red Box), GISP2 and cores VM 28-14 and VM29-191 (Bond et al. 1997) presented alongside the principal surface currents: NAC, North Atlantic Current; IC, Irminger Current; NC, Norwegian Current; EGC, East Greenland Current and EIC, East Iceland Current. (b) Location map detailing the catchment topography and seabed bathymetry with the sampling site of core MD04-2832.

Loch Sunart's catchment and the surrounding areas have a long record of human occupation (e.g. Smout. 1993; Tipping. 2013) extending back to the early Viking presence (~850 AD) and events which potentially caused regional environmental disturbance, such as the intensification of grazing (1350 AD), wide-spread woodland removal (1400-1600 AD), the introduction of lead mining (1722 AD) and start of industrial forestry (1919 AD). Key events in the catchment's history are summarized in Figure 2.

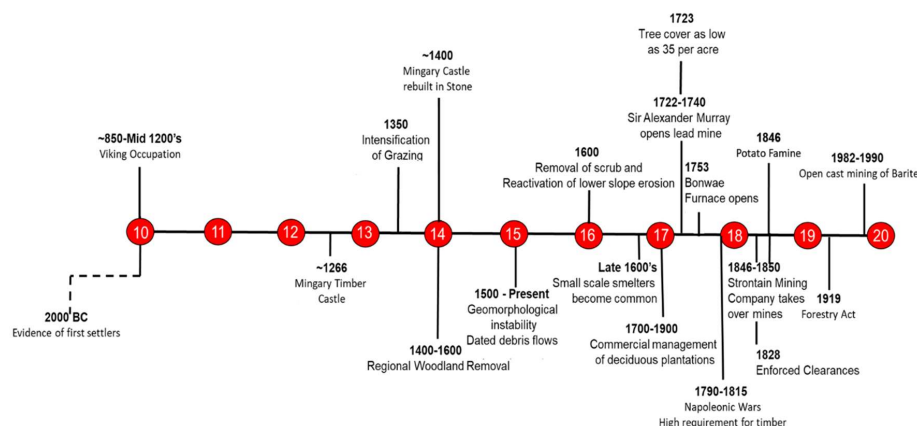


Figure 2. Timeline of key events pertaining to human occupation and disturbance in the Sunart region. Based upon Smout (1993) and Tipping (2013).

2.1 Regional Climate and Oceanography

The northward transport of warm, salty surface waters in the North Atlantic which is a fundamental element of the AMOC and one that asserts a fundamental control upon NW European climate. Flowing into Nordic Seas, the warm surface waters cool and sink promoting the formation of deep-water, which flows back into the Atlantic across the Greenland-Iceland-Scotland Ridge, becoming a major component of North Atlantic Deep Water (NADW). The surface NAC element of the AMOC draws waters from both the cold, fresh subpolar (SPG) and warm, saline subtropical (STG) gyres during its northward flow (Fig. 1). Relative contributions from these two gyres change through time and are primarily controlled by the dynamics of the SPG. Strong SPG circulation provides colder, fresher water to the NAC whilst weaker SPG circulation decreases its contribution to the NAC therefore making it warmer and saltier via enhanced STG contribution.



141 3. Materials and Methods

142 3.1 Sampling

143 A 22.5 m giant piston core MD04-2832 (56.669833, -5.868667) was collected from the
 144 research vessel *Marion Dufresne* in the middle basin of Loch Sunart in 2004 (Fig.1). In addition
 145 to core MD04-2832, a 6m gravity core PM06-GC01 (56.670000, -5.871833) and a multi-core
 146 PMO6 MC01 (56.670000, -5.871667) were collected from the research vessel *Prince Madog*
 147 at same site in 2006. Core MD04-2832 is characterised by stiff silty mud with very little change
 148 throughout its 22.5m length, detailed sedimentological description and photographs can be
 149 found in the supplementary material.

150 3.2 Core Chronology

151 *In-situ* paired bivalve shells (*Corbula varicorbula* and *Nucula sulcata*) were collected from the
 152 length of the core for Accelerator Mass Spectrometry (AMS) dating. In total 22 samples
 153 underwent ^{14}C measurement from MD04-2832, PM06-GC01 and PM06-MC01C (Sup Table.1).
 154 Ages were calibrated using OxCal 4.2.4 (Bronk Ramsey and Lee, 2013) with the Marine13
 155 curve (Reimer, 2013) and a regional correction of ΔR value of -26 ± 14 yr (Cage et al., 2006).
 156 Additionally, a ^{210}Pb chronology was developed for core PM06-MC01 (Sup Table.2). The ^{210}Pb
 157 dating was carried out in Copenhagen University following the Appleby and Oldfield (1992)
 158 and Appleby (2001) methodology. The ^{210}Pb and ^{14}C ages were combined to create a full
 159 chronology for core site MD04-2832. The methodology used magnetic susceptibility and
 160 geochemical (zinc) signatures to splice these core chronologies, this methodology is fully
 161 discussed in Cage and Austin (2010). To further test the splicing two calibrated ^{14}C ages were
 162 acquired from benthic foraminiferal (multi-species) samples from depths of 305cm and 440cm
 163 which agree well with adjacent mollusc shell dates (Sup Table 1), suggesting that the reworking
 164 of older sediment and foraminifera is not a significant problem.



165 An age model was created using the BACON software (Blaauw and Christensen, 2011)
166 representing the 8000 year record (Sup Fig.3). The calibrated model for site MD04-2832 shows
167 that the last 1000 years is contained within the uppermost 280 cm of the sediment record, which
168 has a resolution of $\sim 1 \text{ yr cm}^{-1}$ for the top 50 cm and $4\text{--}6 \text{ yr cm}^{-1}$ for the remainder of the core.

169 **3.3 Geochemical Analysis**

170 Elemental (OC, N) and isotope analyses ($\delta^{13}\text{C}_{\text{org}}$) of the sediments were carried out. Briefly,
171 the samples were dried at 60°C for 24 hours, milled to a powder, with $\sim 12 \text{ mg}$ placed into both
172 tin and silver capsules. The tin capsules were analysed to determine N concentration while the
173 silver capsules undergo acid fumigation (Harris et al., 2001) to remove carbonate. Acid
174 fumigation involves placing the silver capsules in a desiccator with a beaker of 12 M HCl for
175 8hrs to remove carbonate and prevent the loss of water soluble C. Prior to analysis these
176 samples were dried at 60°C for 24 hours. Measurements were made using an elemental analyser
177 interfaced with an isotope ratio mass spectrometer (IRMS). C and N isotope ratios were
178 calculated in δ notation relative to the Vienna Pee Dee Belemnite (VPDB) and Air standards
179 respectively.

180 **3.4 Physical Properties Analysis**

181 Water content, wet and dry bulk density and porosity of the sediment were measured at 10 cm
182 intervals following standard methods (Dadey et al., 1992; Danielson, 1986). Magnetic
183 susceptibility (SI units) measurements were taken at 2 cm resolution. Particle size analysis
184 (PSA) was undertaken, where the organic and carbonate fractions are removed by Hydrogen
185 Peroxide (H_2O_2) and Hydrochloric Acid (HCl) treatments, respectively. The treated samples
186 were then analyzed by laser granulometry using a Beckman Coulter LS230 to measure the
187 particle size ($< 2 \text{ mm}$) of the remaining mineralogical fraction.



188 Sedimentation rates (cm yr^{-1}) were calculated using the output from the Bayesian age-depth
 189 model. OC accumulation rates (OCAR) were calculated using the approach outlined in Smith
 190 et al., (2015). Briefly, the average bulk density, porosity and % OC was calculated allowing
 191 the OCAR to be calculated as follows:

$$192 \quad \text{OCAR} = \% \text{OC} \times \text{sedimentation rate} \times (1 - \text{porosity}) \times \text{bulk density}$$

193 **3.5 Biomarkers**

194 Analysis of alkanes and fatty acids was based on a modified method of Cui et al. (2016b).
 195 Briefly, ~1 g samples were extracted on accelerated solvent extractor (ASE) using
 196 dichloromethane (DCM): methanol (MeOH) (9:1 v:v). After being saponified with KOH in
 197 MeOH, “neutral” and “acid” fractions were sequentially extracted with hexane and
 198 hexane:DCM (4:1 v:v). The former fraction containing alkanes were analysed on the gas
 199 chromatographer – flame ionization detector (GC-FID) for alkane concentrations. The latter
 200 fraction containing fatty acids (FA) were then derivatized using boron trifluoride (BF_3) in MeOH,
 201 re-extracted using DCM, and eluted using DCM on a Pasteur pipette column. Fatty acid methyl
 202 ester (FAME) samples were analysed on the same GC-FID as above.

203 The concentrations of alkanes and fatty acids were calculated and corrected with internal
 204 standards (C_{34} alkane isomer, C_{19} FA) and mix standards of alkanes and FAMES. $\text{ALK}_{\text{C}_{25-35}}$ is
 205 calculated as the sum of the odd chain C_{25} to C_{35} alkanes, while $\text{ALK}_{\text{C}_{24-36}}$ is the sum of even
 206 chain C_{24} to C_{36} alkanes. ALK P_{aq} is the ratio of C_{23} and C_{25} alkanes over the sum of C_{23} , C_{25} ,
 207 C_{29} , C_{31} alkanes. Short-chain fatty acids (SCFA) is calculated as the sum of C_{12} to C_{18} fatty
 208 acids, while long-chain fatty acids (LCFA) is calculated as the sum of C_{24} to C_{32} fatty acids.
 209 Terrestrial to aquatic ratios of fatty acids (TARFA) is the ratio of C_{24} , C_{26} and C_{28} fatty acids
 210 over the sum of C_{12} , C_{14} , C_{16} , C_{24} , C_{26} , C_{28} . Finally, the ratio of fatty acids to alkanes (FA/ALK)
 211 is the ratio of C_{24-32} fatty acids to C_{24-36} alkanes.



212 Analysis of glycerol dialkyl glycerol tetraethers (GDGTs) was based on the method of Liu et
 213 al. (2016) and Smith et al. (2010). Shortly, ~1 g of sediment samples were sonicated and
 214 extracted using DCM: MeOH (9:1 v:v) using an ultra-sonicator. The extracts were re-
 215 concentrated in hexane and analysed on a liquid chromatographer – mass spectrometer (LC–
 216 MS). Quantification of GDGTs was achieved by using a synthesized tetraether surrogate
 217 standard and focusing on targeted ions (e.g., m/z 1292) on the LC–MS. Branched/isoprenoid
 218 tetraether (BIT) index is calculated as the ratio of three branched GDGTs (I, II, and III) to the
 219 sum of branched and crenarchaeol GDGTs. The targeted m/z of the four compounds are 1022,
 220 1036, 1050, and 1292 for branched I, II, III and crenarchaeol GDGTs.

221 3.6 Paleoclimate and Paleo-Environmental Reconstruction

222 Stable oxygen ($\delta^{18}\text{O}$) isotopes were measured on between 20-30 hand-picked individuals of the
 223 infaunal benthic foraminifera species *Ammonia beccarii*. Samples were cleaned in ethanol,
 224 dried at 40°C and run on a Gas-bench coupled to an IRMS. Stable isotope compositions are
 225 reported relative to the Vienna Pee Dee Belemnite (VPDB) using the NBS-19 standard with
 226 precision of 0.07‰ based on an internal Carrara marble standard.

227 We estimate past regional vegetation composition using the regional estimates of vegetation
 228 abundance from large sites (REVEALS) modelling approach (Sugita, 2007). REVEALS is a
 229 Landscape Reconstruction Algorithm (LRA) (Sugita, 2007) which transforms pollen
 230 proportions into estimates of vegetation cover. REVEALSinR implements the REVEALS
 231 model (Theuerkauf et al., 2016) and integrates Lagrangian stochastic dispersal modelling
 232 (Kuparinen et al., 2007). Data for Gallanech Beg were taken from the European Pollen
 233 Database, the site was chosen due to its proximity to our study site and strong chronological
 234 constraint.



235 To estimate the proportion of terrestrial OC in the sediments a mixing model approach was
 236 utilised. The approach used $\delta^{13}\text{C}_{\text{org}}$, $\delta^{15}\text{N}$, C/N ratios and BIT index as tracers in conjunction
 237 with a Bayesian mixing model. The methodological approach used by Smeaton and Austin
 238 (2017) was utilised alongside the OC source characteristics, which are specific to Loch Sunart
 239 (Sup Table 3). This approach does not completely overcome the problems associated with post-
 240 depositional alteration of the organic matter, but the use of four tracers, site specific source
 241 data and a Bayesian approach gives us confidence in the estimates and associated errors to be
 242 largely representative of the sedimentary environment.

243

244 **4. Regional Climate Reconstruction**

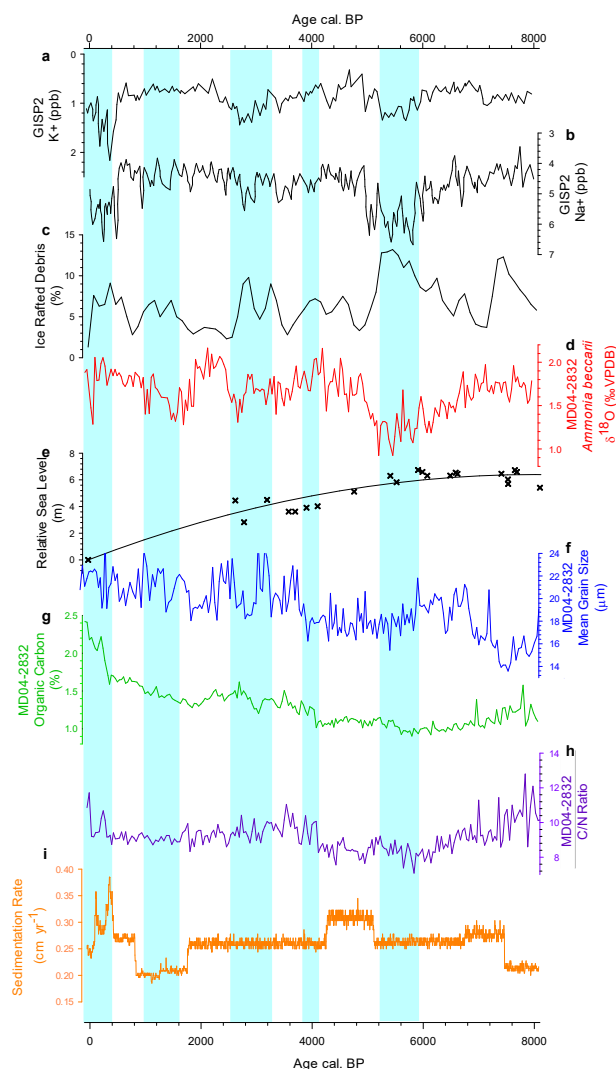
245 Loch Sunart is separated from the coastal ocean by a sill at a water depth of 33 m, which allows
 246 for direct sub-surface exchange and communication of shelf salinity and temperature into the
 247 main basin (Gillibrand et al., 2005). The middle basin core site (MD04-2832) is therefore
 248 directly influenced by the hydrography of the Scottish Shelf, where northward flowing Scottish
 249 Coastal Current (SCC) waters are influenced by the intrusion of North Atlantic water onto the
 250 shelf (Inall et al. 2009). The $\delta^{18}\text{O}$ composition of benthic foraminifera is a measurement of the
 251 interplay between the salinity and temperature of seawater (Cage and Austin, 2010). The
 252 Holocene $\delta^{18}\text{O}$ values of benthic foraminifera at core site MD04-2832 exhibit pronounced
 253 millennial-scale variability of up to 1 ‰ around a long-term average of 1.65 ‰. Values range
 254 from greater than 2 ‰ to less than 1 ‰, indicating changes from colder and/or more saline
 255 conditions to warmer and/or fresher conditions, respectively (Fig.3). Based on the palaeo-
 256 temperature equation O'Neill (1969) and assuming no change in salinity, the observed
 257 Holocene shifts in $\delta^{18}\text{O}$ equate to temperature changes of approximately 4°C. In contrast,
 258 assuming no change in temperature, the observed Holocene 1 ‰ shifts in $\delta^{18}\text{O}$ equate to salinity



259 changes of ~5.5 practical salinity units (psu). Such large and sustained changes in main basin
260 salinity are unlikely, given that coastal salinity changes are small (<0.5) over the instrumental
261 period and that modelling studies (assuming constant coastal salinity boundary conditions)
262 show main basin salinity changed by less than 0.02 during recent extreme NAO years
263 (Gillibrand et al., 2005).

264 The most pronounced feature of the Loch Sunart climate record occurs shortly after 6000 cal.
265 BP, when $\delta^{18}\text{O}$ values reach their most depleted (0.9 ‰) and then increase abruptly shortly
266 before 5000 cal. BP (Fig 3). The timing of this event is broadly coincident with the decreasing
267 relative NADW contribution inferred from benthic foraminiferal $\delta^{13}\text{C}$ from Ocean Drilling
268 Project Site 980, located at a water depth of 2.1 km on the Feni Drift (Fig.1), which began at
269 ~6.5 cal. BP (Oppo et al. 2003). This event is also broadly time equivalent to reconstructions
270 of warmer and more saline surface water inflows to the sub-polar northeast North Atlantic,
271 suggesting that as NADW formation and the strength of the SPG weakened the STG
272 contribution to the NAC (Thornalley et al. 2009). At the same time, chemical records from the
273 Greenland Ice Sheet Project 2 (GISP2) ice core suggest major atmospheric reorganization
274 (Meeker and Mayewski, 2002), with the expansion of the polar vortex and a shift towards
275 winter-like conditions at high latitudes (Fig.3).

276 This coincides with an increase in the relative abundance of haematite-stained grains in
277 northeast North Atlantic cores during this 5-6 kyr event (Bond et al. 2001) which suggests that
278 cold, fresh, ice-bearing surface waters expanded southwards from North of Iceland and were
279 able to influence the strength of SPG circulation. The dynamics of the SPG are therefore critical
280 to AMOC variability and the Loch Sunart $\delta^{18}\text{O}$ data suggest a progressive strengthening
281 (warming) of the STG contribution to the NAC in the build-up to the 5-6 cal. BP event
282 (Thornalley et al. 2009).



283

284 **Figure 3.** Age calibrated MD04-2832 record in the context of North Atlantic Holocene285 paleoclimate records (a) Gaussian smoothed (200 yr) GISP2 sodium (Na^+ ; parts per billion,286 ppb) ion proxy for the Icelandic Low (b) Gaussian smoothed (200 yr) GISP2 potassium (K^+ ;

287 ppb) ion proxy for the Siberian High (Mayewski et al., 2004; Meeker and Mayewski, 2002).

288 (c) Pervasive millennial-scale cycle illustrated by ice-rafted debris (%) from cores VM-28-14

289 and VM-29-191 (Bond et al., 2001). (d) MD04-2832 foraminifera (*Ammonia beccarii*) $\delta^{18}\text{O}$ (‰



290 VPDB) record as a proxy for basin temperature/salinity. (e) Regional relative sea level
291 (Shennan et al., 2005) (f) MD04-2832 mean grain size (after removal of organic and carbonate
292 components) (g) MD04-2832 organic carbon (%) (h) MD04-2832 C/N ratio. (i) Sedimentation
293 rate (cm yr^{-1}) calculated from the Bayesian age model (Sup Fig.3). Vertical shading represent
294 the Rapid Climate Change timing tuned to the GISP2 chronology (Mayewski et al., 2004)



295 **5. Long-term Evolution of a Sedimentary C Store**

296 **5.1 Early to Mid-Holocene**

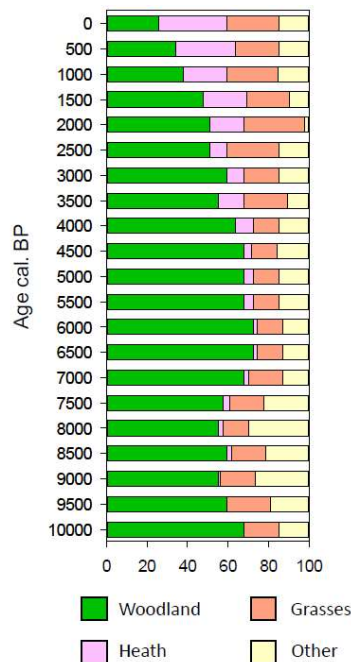
297 During the early to mid-Holocene the accumulation of sediments and the development of the
 298 sedimentary C store is partly governed by ongoing post-glacial Relative Sea Level (RSL)
 299 change. The relatively steady, long-term fall in Holocene RSL (Fig. 3) since 7500 cal. BP
 300 (Shennan et al. 2005) reduced sill depth from ~41 m (early to mid-Holocene) to 33 m (present)
 301 and modified sub-surface exchange and bottom currents with the coastal waters. The increased
 302 openness of the fjord in the early Holocene allowed greater exchange between the coastal and
 303 fjord waters, resulting in a greater proportion of marine derived OC being buried, as illustrated
 304 by the lower C/N ratios found during the early to mid-Holocene (Fig.3). Falling RSL over the
 305 entire Holocene may have gradually restricted the input of marine derived OC and allowed for
 306 the relative increase in the proportion of terrestrial OC; changes in C/N ratio and the coarsening
 307 of mean grain size throughout the Holocene may well reflect these RSL drivers (Fig.3).

308 Climate reorganizations, such as those recorded in the sedimentary record of Loch Sunart, are
 309 likely to have triggered a terrestrial ecosystem response (Frank et al., 2015), in turn increasing
 310 the proportion of terrestrial OC input to the fjord. During the early to mid-Holocene the C/N
 311 ratio remains relatively stable which indicates little or no change in the sources of OC,
 312 suggesting that there was no or only a minor terrestrial ecosystem response to the major climate
 313 reorganizations. Regional landscape vegetation reconstructions (Fig.4) further support this
 314 conclusion - during this period the woodland coverage remained stable and did not respond to
 315 millennial-scale climate reorganizations, as shown by previous pollen analysis from the
 316 neighbouring Loch Etive (Cundill and Austin 2010).

317



318



319

320 **Figure 4.** Estimated Holocene regional vegetation cover types for Gallanech Beg (Davies,
321 2009) a bog 40 km South of Loch Sunart derived from the REVEALS modelling. Pollen
322 counts available from the European Pollen Database (www.europeanpollendatabase.net).

323 5.2 Mid- to Late Holocene

324 The west coast of Scotland has been occupied since the Mesolithic period (Bishop et al. 2015)
325 and it is believed that the region surrounding Loch Sunart was permanently settled at
326 approximately 4000 cal. BP (Tipping 2013; Bishop et al. 2015). The earliest anthropogenic
327 alteration to leave a lasting legacy on the environment was the removal of woodlands (Smout
328 1993). The Gallanech Beg record (Fig.4) shows a decline in woodland cover from 4500 cal.
329 BP, corresponding to the start of a long-term gradual increase in OC content (weight %) in the



330 fjord sediments (Fig. 3). The removal of these woodlands initiated landscape reorganization of
331 vegetation with the appearance of more pioneering plant species and grasslands, which initially
332 dominated the deforested landscape before being replaced by lowland heath plants (Fig. 4).
333 This succession of vegetation is common throughout Scotland and the North Atlantic region
334 (Fyfe et al. 2013). Heath plants, such as heather, have the ability to stabilize soils (Panagos et
335 al. 2015), but are vulnerable to grazers (i.e. sheep and deer) and less adaptable to climate
336 alterations compared to the earlier pioneering plant species (Hartley & Mitchell 2005). The
337 mid- to Late Holocene is characterized by slightly coarser sediment and a gradual increase in
338 C/N ratios, which coincide with periods of rapid North Atlantic climate oscillations (Fig. 3).
339 We hypothesize that the gradual underlying change in vegetation cover superimposed by these
340 rapid shift in the North Atlantic climate may have facilitated the erosion of terrestrial C and its
341 transfer to the marine environment.

342 The mid-Holocene, from around 5000 to 2000 cal. BP, is characterized by largely stable OC
343 accumulation rates (OCAR) (Fig 5a). To maintain this stability in OCAR, we speculate (but
344 cannot prove) that a decrease in marine OC input due to falling sea level may have been
345 balanced by an increase in terrestrial OC input due to natural and anthropogenically induced
346 vegetation change (Fig.4). Previous estimates from Loch Sunart of Holocene OCAR ranged
347 between 1.89 and 25.68 g C m⁻² yr⁻¹ (Smeaton et al., 2016) with the upper range of these
348 estimates originating from the vicinity of core MD04-2832. In comparison to the published
349 values, the OCAR of the early Holocene (8-6 kyrs BP) are significantly higher (38 ± 6 g C m⁻²
350 yr⁻¹), but still fall within the range of OCAR observed in non-glaciated North Atlantic fjords
351 (Smeaton et al., 2016). By the mid to late Holocene (6-1 cal. kyrs BP) the OCAR in MD04-
352 2832 decreased to 26 ± 3 g C m⁻² yr⁻¹ which is equivalent to the rates observed in previous
353 studies at this location within the fjord (Smeaton et al. 2016). This millennial-scale record of
354 OCAR suggests that Loch Sunart has been a hotspot for the burial and storage of C throughout



the Holocene, highlighting the long-term significance of fjords as globally important environments for C burial (Smith et al. 2015).

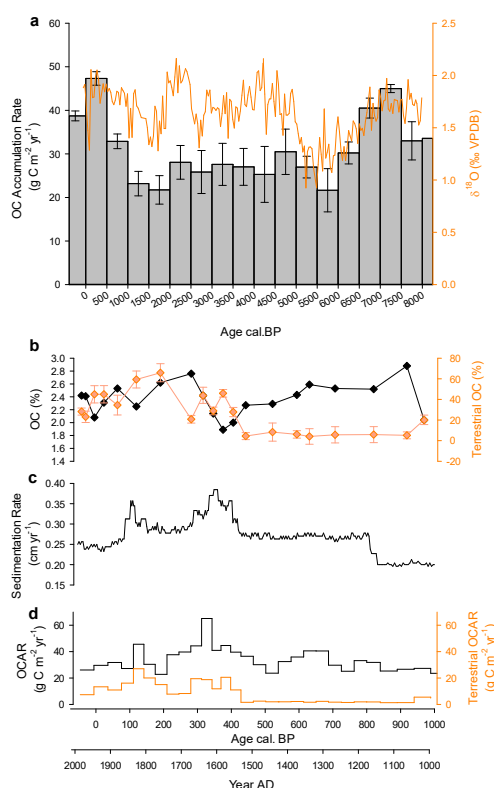


Figure 5. (a) Holocene OC accumulation rates with standard deviation for site MD04-2832
 overlain by the foraminifera $\delta^{18}\text{O}$ record and records for the last millennium (b) % OC and %
 terrestrial OC with uncertainties (c) Sedimentation rate and (d) OCAR and terrestrial OCAR.



5.3 The Last Millennium

The last millennium witnessed a 48 % rise in OCAR above the mid-Holocene average of the preceding 6500 years; these late Holocene OCARs are similar to those observed between 7500-6500 cal. BP. During the last millennium the concentration of marine OC has remained stable, as indicated by constant crenarchaeol concentrations (Sup Fig. 5) suggesting that the increase in OCAR in Loch Sunart's sediment are primarily driven by changes in terrestrial inputs (Fig. 5d). The observed increases in terrestrial OC (Fig. 5b) do not directly correspond to any major change in climate (Fig.3) and RSL change had slowed significantly by this time (Shennan et al., 2005). Therefore the increase in terrestrial OC seems to be de-coupled from either driver (i.e. climate, RSL), suggesting another mechanism had become dominant during this period of time. The last millennium witnessed an unprecedented anthropogenic pressure on the catchment to provide resources for a growing local and national population in Scotland (Sup Fig. 6). Our sediment records show that anthropogenic disturbances to the catchment were initiated at approximately 1520 ± 63 AD, when there is a significant increase in terrestrial input (Fig. 6). Between 1000 – 1520AD, terrestrial OC rose from less than 5% to a maximum of 70% by 1520AD. During this time period (16th Century) scrub vegetation was being removed from the landscape to improve grazing and to supply local charcoal production (Tipping 2013), which in turn reactivated lower slope erosion (Brazier and Ballantyne 1989), the mobilization and transport of soil materials to the loch. It should also be noted that earlier slope instability during the 15th Century and recorded nearby was also likely due to phased woodland and scrub removal (Ballantyne 1991).

In Loch Sunart, the initial phase of the 16th Century disturbance resulted in a pulse of coarse grained mineralogical material being delivered to the sediments, most likely due to the erosion of deep soils (Brazier & Ballantyne 1989; Ballantyne 1991); an observed increase in grain size



386 and magnetic susceptibility is noted at this time (Fig. 6). This high mineralogical input resulted
387 in a dilution effect, lowering the OC in the fjord sediment. The initial pulse was followed by
388 an increased input of terrestrial OC (1584 ± 58 AD), as evidenced by a decrease in $\delta^{13}\text{C}_{\text{org}}$ from
389 -18.5‰ to -25.0‰ and an increase in C/N from 10.5 to a peak of 16.8 (Fig.6). This pattern is
390 comparable to a similar record in Loch Etive (Nørgaard-Pedersen et al. 2006), where in the last
391 1000 years there is a marked increase in OC coupled to an increase in magnetic susceptibility
392 which is indicative of higher mineralogical input suggesting a terrestrial source. This shift
393 towards greater terrestrial input (Fig. 5b) is further supported by the biomarker profiles which
394 all indicate an increase in terrestrial OC input to the sediments (Fig.6), these complementary
395 records are presumably reflecting regional terrestrial responses across NW Scotland.

396 A decline in terrestrial C inputs to Loch Sunart sediments in the early to mid-1800's suggests
397 the fjord system is potentially returning to pre-1520 conditions based on chemical biomarkers
398 and bulk OC proxies. This change could be due to the exhaustion of erodible soil materials, or
399 more likely that the depopulation of the catchment during the 19th century allowed the recovery
400 of vegetation and stabilization of the soils within the catchment. More recent disturbance of
401 the catchment has also impacted the quantity of C held within fjord sediments. In particular,
402 widespread planting of coniferous woodland during the 1950's is associated with increased
403 terrestrial inputs from this time onward (Fig. 6). A pulse of slightly coarser-grained material
404 diluted the bulk OC concentration in the sediments and was followed rapidly (1964 ± 8 AD)
405 by a marked increase in terrestrial OC. Interestingly, this initial response of OC dilution, via
406 coarse lithic material input from eroding soils, is similar to that observed during the 1520 event.

407 The pressure humans have exerted and the associated disturbance of vegetation and soils within
408 the catchment from the late 18th Century to the present day through Lead, Zinc and Copper
409 mining (Sup Fig.7) alongside commercial forestry is several orders of magnitude more intense



410 than prior to the 1520 AD event. For example, the concentrations of these metals increases
411 dramatically from around the mid-1700's, intensifying in the 1900's and corresponds to the
412 written records for mining activity in and around Stontian, within the Loch Sunart catchment
413 (Smout, 1993; Tipping, 2013). Yet the terrestrial response to these later catchment alterations
414 are muted in comparison (Fig. 5). It is therefore unlikely that human activity was the sole driver
415 of this increased terrestrial C storage within the sediments during the 16th Century. Here, we
416 hypothesis that abrupt climatic change may have been the contributing factor responsible for
417 this heightened terrestrial response. For example, at approximately 1525 AD (within
418 chronological uncertainty of 1520 ± 63 AD) there was a rapid reorganization in the NAO
419 recorded in the sediments of Trondheimsfjord, Norway (Faust et al. 2016), where the NAO
420 switched to a positive phase after a sustained period (~315 years) in its negative phase. This
421 positive switch was short (10-15 years) but would have created a wetter atmosphere over NW
422 Europe. Moreover, peatbog water table (Charman et al. 2006; Langdon et al. 2003) and tree
423 ring temperature reconstructions (Rydval et al. 2017) from Scotland confirm this widespread
424 atmospheric reorganization and corroborate a transition to a wetter environment. Loch Sunart
425 has been shown to be sensitive to NAO-forcing (Gillibrand et al. 2005), whereby the switch in
426 the phase of NAO recorded in the $\delta^{18}\text{O}$ record may also have driven increased runoff, and
427 increased C loss through soil erosion. This link between regional climates, oceanography and
428 $\delta^{18}\text{O}$ was outlined in Scottish sea lochs by Cage & Austin (2010) in their interpretation of a
429 millennial-scale record from Loch Sunart. In particular, during the dry negative NAO phases
430 of the Holocene the catchment would build and store soil materials, which could then quickly
431 be lost during the shift to a positive, wetter phase of the NAO. There have, of course, been
432 similar changes to climate and phase of the NAO throughout the Holocene (Fig.3), but not with
433 the same underlying destabilizing effects of humans on the landscape. The major
434 reorganization in the mode of the NAO over the North Atlantic during the late Holocene may



435 have triggered this enhanced terrestrial response. We hypothesize that the long-term
436 modification of the terrestrial environment by humans sensitized the catchment to abrupt
437 climatic reorganization. The shift in the NAO with the associated anthropogenic
438 destabilization resulted in a more vulnerable terrestrial ecosystem, allowing for the
439 mobilization and transfer of terrestrial OC to the fjord sediments (Fig.6).

440 The last millennium has seen two significant increases in sedimentation rate (SR) (Fig. 5c)
441 associated with the 16th century climate event and the post-industrial era (~1850 AD)
442 disturbances of the catchment. Both increases in SR are mirrored by an increase in OCAR;
443 these increases can be large and rapid but they also return to the Holocene background rates
444 within 20-30 years of each major event. This demonstrates that fjords not only record changes
445 in climate and the catchment, but that they also have the capacity to capture and bury OC at
446 greater rate than the long-term Holocene norm (Smeaton et al. 2016). This adaptability of the
447 coastal ocean C, and fjords in particular, in trapping terrestrial OC released by climatic and
448 anthropogenic activities may represent an unrealized yet significant long-term buffer in the
449 global carbon cycle.

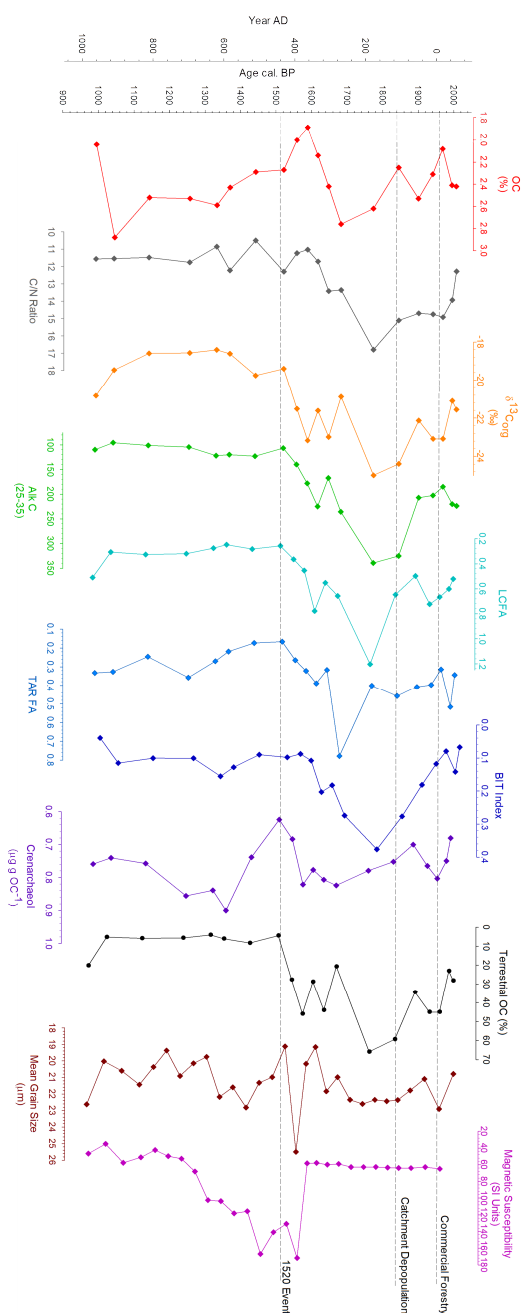


Figure 6. Bulk elemental, biomarker and physical property profiles of core MD04-2832 spanning the last 1000 years. Further biomarker and isotope profiles can be found in the supplementary material.



450 **6. Conclusion**

451 While fjords are known hotspots for C burial (Smith et al. 2015) and storage (Smeaton et al.
452 2016, Smeaton et al., 2017) the effectiveness of these environments as OC sinks over Holocene
453 timescales is now evident from this study. It is clear that both climate and humans are important
454 drivers in the development of such coastal C stores, with the results indicating that both climate
455 change and human activity independently drove changes in the terrestrial environment and
456 transport of OC to the coastal ocean. When climatic and human forcing is coupled, the
457 terrestrial response is heightened. The long-term importance of fjords as hotspots for carbon
458 burial and the potential role of terrestrial carbon subsidy to the coastal ocean as an overlooked
459 component in the global carbon cycle is evident. The capacity of fjords to capture significant
460 quantities of OC and to effectively store both terrestrial and marine C are significantly
461 overlooked services within the earth system.

462

463 **Acknowledgments**

464 This work was finically supported by the Natural Environment Research Council (grant
465 number: NE/L501852/1), the EU FPV HOLSMEER project (EVK2-CT-2000-00060) and the
466 EU FPVI Millennium project (contract number 017008), Biotechnology and Biological
467 Sciences Research Council (grant number: BB/M026620/1) with additional support from the
468 NERC Radiocarbon Facility (Allocation 1154.1005). We acknowledge Jon L. and Beverly A.
469 Thompson Endowed Chair of Geological Sciences held by T.S. Bianchi in the Dept. of
470 Geological Sciences at University of Florida, and China Scholarship Council for supporting
471 part of this research. Further we thank both the SAGES (Scottish Alliance for Geoscience,
472 Environment, Society) and MASTS (The Marine Alliance for Science and Technology for
473 Scotland) pooling initiatives in funding this collaborative research. The CALYPSO long core



474 was acquired by W. Austin within the frame of the French ECLIPSE programme with
475 additional financial support from NERC, SAMS and the University of St Andrews. W. Austin
476 and J. Howe would like to thank Marion Dufresne's Captain J.M. Lefevre, the Chief Operator
477 Y. Balut (from IPEV). Lastly, we would like to thank Charlie Wilson (Scottish Association of
478 Marine Science) and Chris Wurster (University of St-Andrews) for laboratory support.

479

480 **Author Contribution**

481 C.S and W.E.N.A conceived the research and wrote the manuscript in collaboration with T.S.B
482 to which all co-authors contributed data and provided input. The analytical work was
483 undertaken by C.S, X.C and A.G.C under the supervision of W.E.N.A, J.A.H and T.S.B.

484

485

486

487

488

489

490

491

492

493

494

495

496

497

498

499



500 **References**

- 501 Appleby, P.G.: Chronostratigraphic techniques in recent sediments, W.M. Last, J.P. Smol
502 (Eds.), *Tracking Environmental Change Using Lake Sediments, Basin Analysis, Coring and*
503 *Chronological Techniques*, vol. 1, Kluwer Academic Publishers, The Netherlands, pp. 171-
504 203, 2001
- 505 Appleby, P.G, Oldfield, F.: Application of Lead-210 to sedimentation studies, M. Ivanovich,
506 R.S. Harmon (Eds.), *Uranium-series Disequilibrium*, Oxford Science Publication, pp. 731-
507 778, 1992.
- 508 Austin, W.E.N., Cage, A.G. & Scourse, J.D.: Mid-latitude shelf seas: a NW European
509 perspective on the seasonal dynamics of temperature, salinity and oxygen isotopes. *The*
510 *Holocene*, 16(2006), pp.937–947, 2006.
- 511 Ballantyne, C.K.: Late Holocene erosion in upland Britain: climatic deterioration or human
512 influence? *Holocene*, 1(1), pp.81–85, 1991.
- 513 Bishop, R.R., Church, M.J. & Rowley-Conwy, P.A.: Firewood, food and human niche
514 construction: The potential role of Mesolithic hunter-gatherers in actively structuring
515 Scotland's woodlands. *Quaternary Science Reviews*, 108, pp.51–75, 2015.
- 516 Blaauw, M. & Christensen, J.A.: Flexible paleoclimate age-depth models using an
517 autoregressive gamma process. *Bayesian Analysis*, 6(3), pp.457–474, 2011
- 518 Bond, G., Kromer, B., Beer, J., Muscheler, R., Evans, M.N., Showers, W., Hoffmann, S., Lotti-
519 Bond, R., Hajdas, I. and Bonani, G.: Persistent solar influence on North Atlantic climate during
520 the Holocene. *Science*, 294(5549), pp.2130–2136, 2001
- 521 Brazier, V. & Ballantyne, C.K.: Late Holocene debris cone evolution in Glen Feshie, western
522 Cairngorm Mountains, Scotland. *Transactions of the Royal Society of Edinburgh: Earth*
523 *Sciences*, 80(1), pp.17–24, 1989.
- 524 Bronk Ramsey, C. and Lee, S.: 2013. Recent and Planned Developments of the Program OxCal.
525 *Radiocarbon*, 55(2), pp.720–730, 2013.
- 526 Burrell, D. C.: Carbon flow in fjords. *Oceanogr. Mar.Biol. A. Rev.* 26: 143-226, 1988
- 527 Cage, A. G., Heinemeier, J., and Austin, W. E. N.: Marine radiocarbon reservoir ages in
528 Scottish coastal and fjordic waters, *Radiocarbon*, 48, 31–43, 2006
- 529 Cage, A. G. & Austin, W.E.N.: Marine climate variability during the last millennium: The Loch
530 Sunart record, Scotland, UK. *Quaternary Science Reviews*, 29(13–14), pp.1633–1647.
531 Available at: <http://linkinghub.elsevier.com/retrieve/pii/S0277379110000168>, 2010.
- 532 Charman, D.J., Blundell, A., Chiverrell, R.C., Hendon, D. and Langdon, P.G.: Compilation of
533 non-annually resolved Holocene proxy climate records: Stacked Holocene peatland palaeo-
534 water table reconstructions from northern Britain. *Quaternary Science Reviews*, 25(3–4),
535 pp.336–350, 2006.



- 536 Cohen, K.M., MacDonald, K., Joordens, J.C., Roebroeks, W. and Gibbard, P.L.: The earliest
537 occupation of north-west Europe: A coastal perspective. *Quaternary International*, 271(January
538 2015), pp.70–83, 2012.
- 539 Cui, X., Bianchi, T.S., Savage, C. and Smith, R.W.: Organic carbon burial in fjords : Terrestrial
540 versus marine inputs. *Earth and Planetary Science Letters*, 451, pp.41–50. Available at:
541 <http://dx.doi.org/10.1016/j.epsl.2016.07.003>, 2016a.
- 542 Cui, X., Bianchi, T. S., Hutchings, J. A., Savage, C., & Curtis, J. H.: Partitioning of organic
543 carbon among density fractions in surface sediments of Fiordland, New Zealand. *Journal of*
544 *Geophysical Research: Biogeosciences*, 121, 1016–1031, 2016b.
- 545 P.R. Cundill, P.R., Austin, W.E.N.: Pollen analysis of Holocene sediments from Loch Etive, a
546 Scottish fjord. J.A. Howe, J.A., Austin, W.E.N., Forwick, M. Paetzel., M. (Eds.), *Fjord*
547 *Systems and Archives*, The Geological Society, London, Special Publications 344 (2010),
548 pp. 331-340, 2010.
- 549
- 550 Dadey, K.A., Janecek, T. & Klaus, A.: Dry bulk density: its use and determination.
551 *Proceedings of the Ocean Drilling Program, Scientific Results*, 126, pp.551–554, 1992.
- 552 Danielson, R.E. & Sutherland, P.L.: Porosity. In *Methods of soil analysis*, part 1, Physical and
553 mineralogical methods. pp. 443–461, 1986.
- 554 Davies, F., Pollen profile GB4, Gallanech Beg, United Kingdom. European Pollen Database
555 (EPD).
- 556 Faust, J.C., Fabian, K., Milzer, G., Giraudeau, J. and Knies, J.: Norwegian fjord sediments
557 reveal NAO related winter temperature and precipitation changes of the past 2800 years. *Earth*
558 *and Planetary Science Letters*, 435, pp.84–93, 2016.
- 559 Frank, D., Reichstein, M., Bahn, M., Thonicke, K., Frank, D., Mahecha, M.D., Smith, P., Van
560 der Velde, M., Vicca, S., Babst, F. and Beer, C.: Effects of climate extremes on the terrestrial
561 carbon cycle: concepts, processes and potential future impacts. *Global Change Biology*. doi:
562 10.1111/gcb.12916, 2015.
- 563 Fyfe, R.M., Twiddle, C., Sugita, S., Gaillard, M.J., Barratt, P., Caseldine, C.J., Dodson, J.,
564 Edwards, K.J., Farrell, M., Froyd, C. and Grant, M.J.: The Holocene vegetation cover of Britain
565 and Ireland: Overcoming problems of scale and discerning patterns of openness. *Quaternary*
566 *Science Reviews*, 73, pp.132–148, 2013
- 567 Gillibrand, P. A., Cage, A. G. & Austin, W.E.N.: A preliminary investigation of basin water
568 response to climate forcing in a Scottish fjord: evaluating the influence of the NAO.
569 *Continental Shelf Research*, 25(5–6), pp.571–587, 2005
- 570 Harris, D., Horwáth, W.R. & van Kessel, C.: Acid fumigation of soils to remove carbonates
571 prior to total organic carbon or CARBON-13 isotopic analysis. *Soil Science Society of*
572 *America Journal*, 65(6), p.1853, 2001.
- 573 Hartley, S.E. & Mitchell, R.J.: Manipulation of nutrients and grazing levels on heather
574 moorland: Changes in *Calluna* dominance and consequences for community composition.
575 *Journal of Ecology*, 93(5), pp.990–1004, 2005.



- 576 Hinojosa, J.L., Moy, C.M., Stirling, C.H., Wilson, G.S. and Eglinton, T.I.: Carbon cycling and
577 burial in New Zealand's fjords, *Geochem. Geophys. Geosyst.*, 15, 4047–4063, 2014
- 578 Inall, M., Gillibrand, P., Griffiths, C., MacDougall, N. & Blackwell, K.: 'On the oceanographic
579 variability of the North-West European Shelf to the West of Scotland' *Journal of Marine*
580 *Systems*, vol 77(3), no. 3, pp. 210–226. DOI: 10.1016/j.jmarsys.2007.12.012, 2009.
- 581 Keil, R. G. & Mayer, L. M.: in *Treatise on Geochemistry* 2nd edn (eds Holland, H. D. &
582 Turekian, K. K.) 337–359, 2014.
- 583 Kuparinen, A., Markkanen, T., Riikonen, H. and Vesala, T.: Modeling air-mediated dispersal
584 of spores, pollen and seeds in forested areas. *Ecological Modelling*, 208(2–4), pp.177–188,
585 2007.
- 586 Langdon, P.G., Barber, K.E. & Hughes, P.D.M.: A 7500-year peat-based palaeoclimatic
587 reconstruction and evidence for an 1100-year cyclicity in bog surface wetness from Temple
588 Hill Moss, Pentland Hills, southeast Scotland. *Quaternary Science Reviews*, 22(2–4), pp.259–
589 274, 2003.
- 590 Liu, X.L., De Santiago Torio, A., Bosak, T. and Summons, R.E.: Novel archaeal tetraether
591 lipids with a cyclohexyl ring identified in Fayetteville Green Lake, NY, and other sulfidic
592 lacustrine settings. *Rapid Communications in Mass Spectrometry*, 30(10), pp.1197–1205, 2016.
- 593 Mayewski, P.A., Rohling, E.E., Stager, J.C., Karlén, W., Maasch, K.A., Meeker, L.D.,
594 Meyerson, E.A., Gasse, F., van Kreveland, S., Holmgren, K. and Lee-Thorp, J.: Holocene climate
595 variability. *Quaternary Research*, 62(3), pp.243–255, 2004.
- 596 Meeker, L.D. and Mayewski, P. A.: A 1400-year high-resolution record of atmospheric
597 circulation over the North Atlantic and Asia. *The Holocene*, 12(3), pp.257–266, 2002.
- 598 Newer, J.M. and Keil, R.G.: Sedimentary organic matter geochemistry of Clayoquot Sound,
599 Vancouver Island, British Columbia. *Limnol. Oceanogr.*, 50(4), 1119–1128, 2005
- 600 Nørgaard-Pedersen, N., Austin, W. E. N., Howe, J. A., & Shimmield, T. : The Holocene record
601 of Loch Etive, western Scotland: Influence of catchment and relative sea level changes. *Marine*
602 *Geology*, 228(1–4), pp.55–71, 2006.
- 603 O'Neil, J.R., Clayton, R.N., Mayeda, T.: Oxygen isotope fractionation in divalent metal
604 carbonates *Journal of Chemical Physics*, 51 (1969), pp. 5547–5558, 1969.
- 605 Oppo, D., McManus, J. & Cullen, J.L.: Deepwater variability in the Holocene epoch. *Nature*,
606 422(March), p.277, 2003.
- 607 Ortega, P. et al., 2015. Ortega, P., Lehner, F., Swingedouw, D., Masson-Delmotte, V., Raible,
608 C. C., Casado, M., & Yiou, P.: *Nature*, 523(7558), pp.71–74.
- 609 Panagos, P., Borrelli, P., Meusburger, K., Alewell, C., Lugato, E., & Montanarella, L.:
610 Estimating the soil erosion cover-management factor at the European scale. *Land Use Policy*,
611 48, pp.38–50, 2015



- 612 Peeters, J.H.M & Momber, G.: The southern North Sea and the human occupation of northwest
613 Europe after the Last Glacial Maximum, *Netherlands Journal of Geosciences*, 93(1-2) pp.55-
614 70, 2014
- 615 Reimer, P.: IntCal13 and Marine13 Radiocarbon Age Calibration Curves 0–50,000 Years cal
616 BP. *Radiocarbon*, 55(4), pp.1869–1887, 2013
- 617 Rydval, Miloš, Björn E. Gunnarson, Neil J. Loader, Edward R. Cook, Daniel L. Druckenbrod,
618 and Rob Wilson.: Spatial reconstruction of Scottish summer temperatures from tree rings.
619 *International Journal of Climatology*, 37(3), pp.1540–1556, 2017.
- 620 Seddon, A. W., Macias-Fauria, M., Long, P. R., Benz, D., & Willis, K. J.: Sensitivity of global
621 terrestrial ecosystems to climate variability. *Nature*, 531(7593), pp.229–232, 2016
- 622 Shennan I, Hamilton S, Hillier C, Woodroffe S. A.: A 16000-year record of near-field relative
623 sea-level changes, northwest Scotland, United Kingdom. *Quaternary International*, 133–134,
624 pp.95–106. Available at: <http://linkinghub.elsevier.com/retrieve/pii/S1040618204001880>,
625 2005.
- 626 Simo-Matchim AG, Gosselin M, Blais M, Gratton Y, Tremblay JÉ.: Seasonal variations of
627 phytoplankton dynamics in Nunatsiavut fjords (Labrador, Canada) and their relationships with
628 environmental conditions. *Journal of Marine Systems* 156: 56–75, 2016.
- 629 Skei J. M.: Geochemical and sedimentological considerations of a permanently anoxic fjord—
630 Framvaren, south Norway. *Sed. Geol.* 36: 131–145, 1983.
- 631 Smeaton, C., Austin, W. E. N., Davies, A. L., Baltzer, A., Abell, R. E., and Howe, J. A.:
632 Substantial stores of sedimentary carbon held in mid-latitude fjords, *Biogeosciences*, 13, 5771-
633 5787, <https://doi.org/10.5194/bg-13-5771-2016>, 2016.
- 634 Smeaton, C. & Austin, W.E.N.: Sources, Sinks and Subsidies: Terrestrial Carbon Storage in
635 the Coastal Ocean. *Journal of Geophysical Research: Biogeosciences*, 122,
636 doi/10.1002/2017JG003952, 2017.
- 637 Smeaton, C., Austin, W. E. N., Davies, A. L., Baltzer, A., Howe, J. A., and Baxter, J. M.:
638 Scotland's Forgotten Carbon: A National Assessment of Mid-Latitude Fjord Sedimentary
639 Carbon Stocks, *Biogeosciences*, 14, 5663-5674, <https://doi.org/10.5194/bg-14-5663-2017>,
640 2017.
- 641 Smith, R. W., Bianchi, T. S., Allison, M., Savage, C., & Galy, V.: High rates of organic carbon
642 burial in fjord sediments globally. *Nature Geoscience*, 8, 450–453.
643 <https://doi.org/10.1038/NGEO2421>, 2015.
- 644 Smith, R.W., Bianchi, T.S. & Savage, C.: Comparison of lignin phenols and
645 branched/isoprenoid tetraethers (BIT index) as indices of terrestrial organic matter in Doubtful
646 Sound, Fiordland, New Zealand. *Organic Geochemistry*, 41(3), pp.281–290, 2010.
- 647 Smout, T.C.: Scotland since prehistory: Natural change and human impact, Scottish Natural
648 Heritage, Scottish Cultural Press, 1993
- 649 Sugita, S.: Theory of quantitative reconstruction of vegetation I: pollen from large sites
650 REVEALS regional vegetation composition. *The Holocene*, 17, pp.229–241, 2007.



- 651 Syvitski, J.P.M, Burrell, D.C, Skei, J.M.: Fjords: Processes and Products. Springer-Verlag,
652 1987.
- 653 Syvitski, J. P. M. and Shaw, J.: Sedimentology and Geomorphology of Fjords, Geomorphology
654 and Sedimentology of Estuaries, Dev. Sedimento., 53, 113–178, 1995.
- 655 Theuerkauf, M., Couwenberg, J., Kuparinen, A. and Liebscher, V.: A matter of dispersal:
656 REVEALSinR introduces state-of-the-art dispersal models to quantitative vegetation
657 reconstruction. Vegetation History and Archaeobotany, 25(6), pp.541–553, 2016
- 658 Thornalley, D.J.R., Elderfield, H. & McCave, I.N.: Holocene oscillations in temperature and
659 salinity of the surface subpolar North Atlantic. Nature, 457(7230), pp.711–714, 2009
- 660 Tipping, R.: Towards an Environmental History of Argyll & Bute: A Review of Current Data,
661 Their Strengths and Weaknesses and Suggestions for Future Work, 2013
- 662 Zillén, L. & Conley, D.J.: Hypoxia and cyanobacteria blooms - Are they really natural features
663 of the late Holocene history of the Baltic Sea? Biogeosciences, 7(8), pp.2567–2580, 2010.
- 664